Tobias H. Donner, Markus Siegel, Robert Oostenveld, Pascal Fries, Markus Bauer and Andreas K. Engel
J Neurophysiol 98:345-359, 2007. First published May 9, 2007; doi:10.1152/jn.01141.2006

You might find this additional information useful...

Supplemental material for this article can be found at:
http://jn.physiology.org/cgi/content/full/01141.2006/DC1

This article cites 64 articles, 27 of which you can access free at:
http://jn.physiology.org/cgi/content/full/98/1/345#BIBL

Updated information and services including high-resolution figures, can be found at:
http://jn.physiology.org/cgi/content/full/98/1/345

Additional material and information about ***Journal of Neurophysiology*** can be found at:
http://www.the-aps.org/publications/jn

This information is current as of July 27, 2007 .

Journal of Neurophysiology publishes original articles on the function of the nervous system. It is published 12 times a year (monthly) by the American Physiological Society, 9650 Rockville Pike, Bethesda MD 20814-3991. Copyright © 2005 by the American Physiological Society. ISSN: 0022-3077, ESSN: 1522-1598. Visit our website at http://www.the-aps.org/.

Downloaded from jn.physiology.org on July 27, 2007

J Neurophysiol 98: 345–359, 2007.
First published May 9, 2007; doi:10.1152/jn.01141.2006.

Population Activity in the Human Dorsal Pathway Predicts the Accuracy of Visual Motion Detection

Tobias H. Donner,[1,2] Markus Siegel,[1,2] Robert Oostenveld,[2] Pascal Fries,[2,3] Markus Bauer,[2,3] and Andreas K. Engel[1]

[1]*Department of Neurophysiology and Pathophysiology, University Medical Center Hamburg–Eppendorf, Hamburg, Germany; and* [2]*F.C. Donders Centre for Cognitive Neuroimaging; and* [3]*Department of Biophysics, Radboud University Nijmegen, Nijmegen, The Netherlands*

Submitted 26 October 2006; accepted in final form 6 May 2007

Donner TH, Siegel M, Oostenveld R, Fries P, Bauer M, Engel AK. Population activity in the human dorsal pathway predicts the accuracy of visual motion detection. *J Neurophysiol* 98: 345–359, 2007. First published May 9, 2007; doi:10.1152/jn.01141.2006. A person's ability to detect a weak visual target stimulus varies from one viewing to the next. We tested whether the trial-to-trial fluctuations of neural population activity in the human brain are related to the fluctuations of behavioral performance in a "yes–no" visual motion-detection task. We recorded neural population activity with whole head magnetoencephalography (MEG) while subjects searched for a weak coherent motion signal embedded in spatiotemporal noise. We found that, during motion viewing, MEG activity in the 12- to 24-Hz ("beta") frequency range is higher, on average, before correct behavioral choices than before errors and that it predicts correct choices on a trial-by-trial basis. This performance-predictive activity is not evident in the prestimulus baseline and builds up slowly after stimulus onset. Source reconstruction revealed that the performance-predictive activity is expressed in the posterior parietal and dorsolateral prefrontal cortices and, less strongly, in the visual motion-sensitive area MT+. The 12- to 24-Hz activity in these key stages of the human dorsal visual pathway is correlated with behavioral choice in both target-present and target-absent conditions. Importantly, in the absence of the target, 12- to 24-Hz activity tends to be higher before "no" choices ("correct rejects") than before "yes" choices ("false alarms"). It thus predicts the accuracy, and not the content, of subjects' upcoming perceptual reports. We conclude that beta band activity in the human dorsal visual pathway indexes, and potentially controls, the efficiency of neural computations underlying simple perceptual decisions.

INTRODUCTION

One of the most general observations in the study of visual perception is that observers' judgments about the presence of a target stimulus near detection threshold fluctuate from one stimulus presentation to the next. To account for these fluctuations, psychophysical models incorporate random variations (i.e., noise) somewhere between the stimulus and the observer's decision (Graham 1989; Green and Swets 1966). At the neural level, sensory signals have to propagate through several stages of the cortical hierarchy before reaching the motor circuits that ultimately control behavioral responses (Felleman and Van Essen 1991). A major challenge for systems neuroscience is to identify the stages of the visuomotor pathways, and the specific patterns of neural activity therein, that underlie the (fluctuating) psychophysical performance.

Address for reprint requests and other correspondence: T. H. Donner, Department of Psychology and Center for Neural Science, New York University, 6 Washington Place, 8th floor, New York, NY 10003-6634 (E-mail: tobias@cns.nyu.edu).

The firing-rate responses of single cortical neurons vary across repeated presentations of the same visual stimulus (e.g., Buracas et al. 1998; Carandini 2004; Heggelund and Albus 1978). These spike-rate fluctuations predict monkeys' behavioral responses in visual detection and discrimination tasks. This association between firing rates and behavior becomes stronger when proceeding from early visual cortical regions, such as the motion-sensitive area MT, to associative areas in parietal and prefrontal cortex (Britten et al. 1996; Cook and Maunsell 2002; Kim and Shadlen 1999; Shadlen and Newsome 2001; Thiele et al. 1999; Uka and DeAngelis 2004; Williams et al. 2003). Responses of single neurons in visual cortical areas like MT are believed to provide a representation of the sensory evidence (Newsome and Parker 1998), which is integrated over time and transformed into an action plan in posterior parietal and prefrontal cortex (Gold and Shadlen 2001).

At the population level, cortical responses to visual stimuli commonly display a temporal fine structure with a characteristic spectral profile, which is evident both in the intracortical local field potential (e.g., Fries et al. 2001; Gray and Singer 1989; Henrie and Shapley 2005; Siegel and König 2003) and in the scalp electroencephalogram or magnetoencephalogram (EEG or MEG, respectively) (Siegel et al. 2007; Tallon-Baudry and Bertrand 1999). Similar to the average firing rates of single neurons, such population responses exhibit strong trial-to-trial fluctuations (Arieli et al. 1996; Buracas et al. 1998). At present, little is known about the trial-to-trial covariation between cortical population responses and behavioral responses to visual stimuli near detection threshold. Cortical population activity has been measured indirectly in humans with functional magnetic resonance imaging (fMRI) during a variety of visual detection tasks. These studies consistently reported larger fMRI responses in parietal and prefrontal cortex when targets are detected than when they are missed (Beck et al. 2001; Kranczioch et al. 2005; Marois et al. 2004). Specifically, during motion detection, such a pattern of fMRI responses has been observed in the human motion-sensitive V5/MT+ complex (the putative homologue of macaque MT) as well as in parietal cortex (Shulman et al. 2001). However, the fMRI signal provides only limited information about the time course and temporal fine structure of neural activity. Electrophysiological studies are necessary to determine the exact trial interval and the frequency range, in which detection-related modulation of cortical population responses occurs.

Most importantly, it is currently not clear which *aspect* of visual detection decisions is reflected by neural mass activity in the primate parietal and prefrontal cortices: perceptual deci-

0022-3077/07 $8.00 Copyright © 2007 The American Physiological Society

Downloaded from jn.physiology.org on July 27, 2007

sions can be classified according to their *content* and their *accuracy* (Green and Swets 1966). Specifically, perceptual decisions in a simple "yes–no" detection task can be classified according to whether the subject reports "yes, the target is present" or "no, it is not," and whether this report is correct. Both classification schemes overlap for target-present trials. Target-absent trials, however, dissociate these two schemes and can therefore be used to pinpoint the role of a neural activity parameter in the perceptual decision process: If a neural signal reflects the choice *content*, its magnitude should be larger before "yes" than before "no" reports, irrespective of whether the target is physically present. In other words, one should observe: "hits" > "misses" for target-present and "false alarms" > "correct rejects" for target-absent conditions. Such a pattern of neural population activity has been observed in several visual cortical areas in fMRI studies of contrast and face detection (McKeeff and Tong 2007; Ress and Heeger 2003; Summerfield et al. 2006). Alternatively, if a neural signal reflects the *accuracy* of choices, the rank order of activity before "yes" and "no" choices should be opposite in target-present and target-absent conditions. That is, one should then observe: hits > misses and correct rejects > false alarms.

The goal of the present study was to test whether the trial-to-trial fluctuations of frequency specific neural population responses to visual motion in the human "dorsal pathway" (Haxby and Ungerleider 1994) are related to behavioral-detection performance. Specifically, we aimed at determining whether such activity in three key stages of this pathway (MT+, parietal, and prefrontal cortex) predicts the *content* or the *accuracy* of decisions about the presence of motion. We recorded neural population activity with MEG while subjects performed a "yes–no" motion-detection task near psychophysical threshold (Fig. 1). We quantified the link between MEG activity and behavior across a wide range of frequencies (4–100 Hz). We found that the sustained MEG activity in the 12- to 24-Hz ("beta") range during motion viewing, but not before stimulus onset, predicts correct behavioral responses on single trials. This performance-predictive MEG activity builds up slowly during motion viewing and is expressed in prefrontal and posterior parietal cortices and, less robustly, in area MT+. Importantly, in the absence of the target, 12- to 24-Hz activity in all three areas is larger before correct rejects than before false alarms. Thus this activity predicts the accuracy, but not the content, of visual detection decisions.

METHODS

Subjects

Four healthy subjects (all male; age range: 23–30 yr) participated in the study, conducted in accordance with the Declaration of Helsinki. Two of the subjects (MS and THD) are authors. The other two were naive to the purpose of the experiment and were paid for their participation. All subjects were in good health with no history of psychiatric or neurological illness. They had normal or corrected-to-normal vision.

Psychophysics

STIMULI. We used dynamic random dot patterns to stimulate the cortical visual motion system. The stimuli were constructed off-line in MATLAB (The MathWorks, Natick, MA) according to a standard

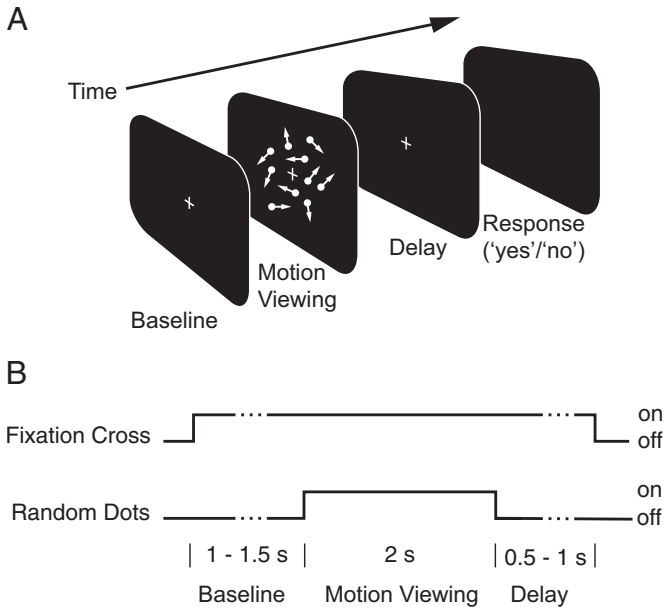

FIG. 1. Visual motion detection task. Illustrations of the intervals and the time course of stimuli within a trial are shown in *A* and *B*, respectively. Trials began with the onset of a red fixation cross. After a baseline period of 1–1.5 s, a dynamic random-dot pattern was presented in the visual field center for 2 s. On each trial, either a weak target pattern (4.5–10.5% motion coherence, adjusted to the individual detection threshold) or a noise pattern (0% motion coherence) was presented. A target occurred on half of the trials. Subjects had to decide whether the target was present. After a variable delay (0.5–1 s), the fixation cross was extinguished, which prompted subjects to indicate their decision ("yes" or "no") by pressing one of two buttons (right or left hand).

procedure (e.g., Britten et al. 1996; Rees et al. 2000). Stimulus presentation was controlled by a personal computer running the Presentation Software (NeuroBehavioral Systems, Albany, CA). Stimuli were projected from a calibrated liquid crystal display (LCD) projector (situated outside the magnetically shielded room) onto a back-projection screen through a tube by a mirror system. The refresh rate of the projector was 60 Hz. The screen was mounted in front of the subject's head. Each frame of the animation consisted of an array of white dots randomly positioned on a black background. Each dot was displaced from frame to frame. Random dot patterns were either target patterns or noise patterns. Noise patterns consisted of dots that were randomly displaced from frame to frame. Target patterns contained a small fraction of dots that were coherently displaced in a common direction, with fixed spatial offset. All other dots were displaced to randomly selected positions. The coherently moving dots were randomly selected afresh on each new frame, that is, their "lifetime" was limited. The level of motion coherence (i.e., the fraction of coherently moving dots) was chosen individually for each subject to correspond to the subject's detection threshold (see following text). The patterns were confined to a circular aperture and centered on a red fixation cross. The diameter of each of the dots on the projection screen was approximately 0.2 deg. Their density and speed were approximately 1.7 deg^{-2} and approximately 11.5 deg/s, respectively. The aperture diameter was about 43 deg.

TASK AND PROCEDURE. Subjects performed a "yes–no" motion coherence detection task. The target occurred on 50% of the trials. Each trial began with the onset of the central fixation crosshair and consisted of three consecutive intervals (Fig. 1): *1*) a prestimulus baseline of variable duration (uniformly distributed between 1,000 and 1,500 ms), *2*) the motion viewing interval (2 s), and *3*) a variable delay (uniformly distributed between 500 and 1,000 ms), after which the fixation cross was turned off. Subjects were instructed to fixate the crosshair throughout the trial, to monitor the whole stimulus pattern,

Downloaded from jn.physiology.org on July 27, 2007

to form a decision about the presence of the target during motion viewing, and to report this decision by pressing one of two response buttons ("yes, target is present" or "no, it is not") with their left or right index finger after the fixation cross offset. Auditory feedback (a beep) was provided after each incorrect response by plastic tubes and earpieces. The subsequent inter-trial interval spanned 900 ms. Subjects were allowed to make eye movements or blinks during the inter-trial interval. The mapping between perceptual decision ("yes"/"no") and response hand (left/right) was counterbalanced across subjects. The delay between stimulus offset and motor response was introduced to dissociate neural activity related to stimulus processing from neural activity related to the execution of the motor response. The stimulus duration of 2 s was chosen in conformity with previous single-unit studies of motion discrimination in monkeys (Britten et al. 1996; Kim and Shadlen 1999; Shadlen and Newsome 2001). Each run consisted of 400 trials and lasted about 50 min.

If present, the target moved either upward or downward. Target absence/presence was randomly selected on each trial, under the constraint that each would occur equally often within a run. On target-present trials, upward/downward was randomly selected, again under the constraint that each direction would occur equally often within a run. Apart from this variation, all stimulus patterns in the MEG recording sessions were exact repeats. This fact was unknown to the naive subjects and informal debriefing verified that it remained unnoticed throughout the series of experimental sessions. Importantly, this procedure enabled us to investigate stimulus-independent trial-to-trial covariations between MEG activity and subjects' detection performance. After blocks of 50 trials, subjects were allowed to pause, without moving their heads. They initiated the start of each new trial block by a button press. Each recording session consisted of between one and three runs (~50 min each), with two runs in the vast majority of sessions. Subjects 1 and 2 each completed 15 runs (6,000 trials). Subjects 3 and 4 each completed eight runs (3,200 trials).

Before the MEG recordings, motion coherence thresholds were individually determined in a two-alternative forced-choice paradigm (upward/downward discrimination) using the method of constant stimuli (Green and Swets 1966). After at least six sessions of around 45 min each, coherence levels yielding roughly 71% correct responses were estimated from a Weibull function fit to the psychometric data. Subjects then performed two sessions of around 30 min with the yes–no detection task at the obtained threshold level of coherence. In these psychophysical sessions, we presented ten different, randomly intermixed variants of each, target and noise stimuli. If performance changed by >5% correct from one session to the next, the coherence level was changed accordingly and a further session was conducted. This procedure yielded stable average performance during the subsequent MEG experiments. The resulting coherence levels, used throughout the MEG recordings, were as follows: 4.5% (subject 1), 5.5% (subjects 2 and 4), and 10.5% (subject 3).

MEG data acquisition

We recorded the MEG (Hamalainen et al. 1993) continuously using a 151-channel whole head system (Omega 2000; CTF Systems, Port Coquitlam, Canada). Subjects were seated in a chair positioned in a magnetically shielded room. The electrooculogram was recorded simultaneously for off-line artifact rejection. MEG signals were low-pass filtered on-line (cutoff: 300 Hz) and recorded with a sampling rate of 1,200 Hz. The head position relative to the MEG sensors was measured before and after each run using small electromagnetic coils positioned at the subject's nasion and at the right and left ear canals. The source analysis and visualization (see following text) required the coregistration of the MEG data with anatomical MRIs of the same subject. Therefore we acquired high-resolution (1 mm^3) structural MRIs on a 1.5-T whole body Magnetom Sonata MRI system (Siemens Medical Systems, Erlangen, Germany) from each subject with a T1-weighted sagittal MP–Rage (magnetization-prepared rapid gradient-echo) sequence.

Data analysis

We used the CTF data analysis software package to construct head models from the structural MRIs. We used the BrainVoyager QX software package (Brain Innovation, Maastricht, The Netherlands) to reconstruct the cortical surfaces, to define regions of interest based on anatomical criteria, and to visualize the MEG source reconstructions. All other data analyses were performed in MATLAB using the open source toolbox "FieldTrip" (http://www.ru.nl/fcdonders/fieldtrip) and additional custom-made software.

PREPROCESSING. Only runs with a head displacement <6 mm (Euclidean distance in 3D space) across the entire recording interval were included in the analysis. Two of 48 runs in total did not meet this criterion. One additional run had to be discarded because of a defect of the LCD projector. We categorized trials according to whether the target was present or absent and whether the subject chose "yes" or "no," yielding the four categories of signal-detection theory (Green and Swets 1966): hits and misses (target present) and false alarms and correct rejects (target absent). We first extracted trials from the MEG time series separately for the four categories and subsequently recombined them in a subset of the analyses (see following text). Trials extended from 500 ms before the onset of the dynamic random-dot patterns to 500 ms after their offset. Artifact rejection for these epochs was performed off-line. Trials containing eye blinks, saccades, muscle artifacts, and signal jumps were rejected from further analysis using semiautomatic procedures. We discarded one "bad" MEG sensor overlying right temporal cortex ("MRT16") from all analyses. Line noise was removed by subtracting the 50-, 100-, 150-, and 200-Hz Fourier components of the individual epochs padded with adjacent data from the continuous recording to 5-s length. Preprocessed data were low-pass filtered at 300 Hz and resampled at 600 Hz. For the analysis of time-averaged responses during baseline and motion viewing, subepochs were further extracted from the trials (see following text).

SPECTRAL ANALYSIS. We used the "multitaper" method for all spectral analyses subsequently described (Mitra and Pesaran 1999). This method provides a trade-off between minimizing bias and variance of spectral estimators on the one hand and maximizing spectral resolution on the other hand. To quantify the strength of stimulus responses at a given center frequency, $\Delta R(f)$, estimators of power spectral density at that frequency, $P(f)$, were converted into units of percentage change from baseline, according to

$$\Delta R(f) = \frac{P(f) - P_b(f)}{P_b(f)} \times 100\% \quad (1)$$

where P_b denotes the average power spectral density in the prestimulus period (starting 500 ms before stimulus onset). Unless stated otherwise, this quantity was used as the measure of the MEG response in the analyses reported herein.

All sensor-level analyses subsequently described focused on a fixed group of 20 posterior MEG sensors (Fig. 2). These sensors displayed robust stimulus responses and covered motion-sensitive areas in dorsal visual and posterior parietal cortex (Siegel et al. 2007). To generate time–frequency representations of the MEG responses, $\Delta R(f, t)$, a "multitaper" sliding window Fourier transform (400-ms window, 8-Hz spectral smoothing, 50-ms window step size) was applied to the individual trials of all categories. The results were magnitude-squared and then averaged across tapers and trials, yielding a time–frequency representation of power for each of the 150 sensors. The resulting spectrograms were collapsed across the 20 sensors of interest and converted to $\Delta R(f, t)$ according to *Eq. 1*. To obtain time–frequency representations of the phase-locked responses

Downloaded from jn.physiology.org on July 27, 2007

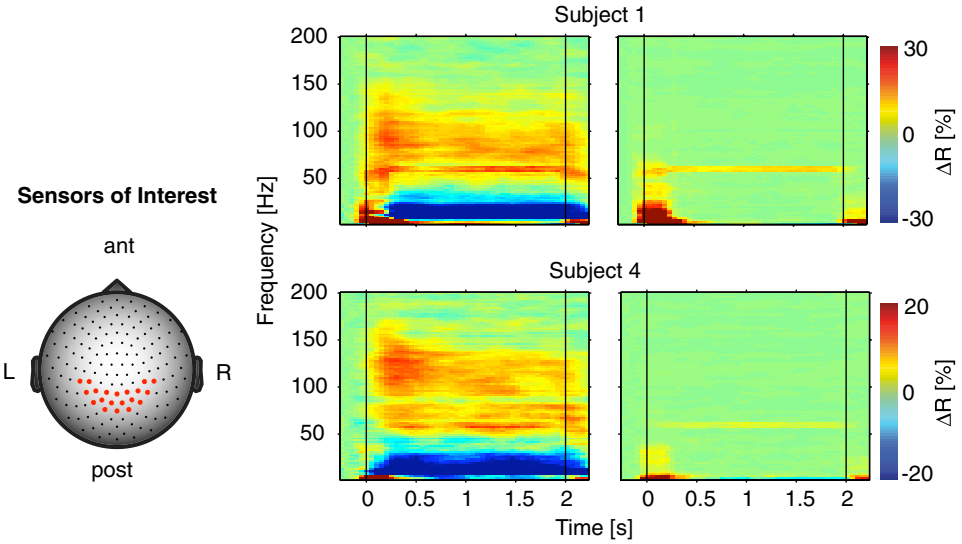

FIG. 2. Magnetoencephalographic (MEG) responses to moving random dot patterns are sustained throughout the stimulus interval. *Bottom left*: 20 posterior sensors contributing to the responses shown on the *right* are marked in red on a 2-dimensional (2D) projection of the sensor array superimposed on a schematic of the head. Time–frequency representations of the MEG response to random-dot patterns (average across all trials) are shown for two representative subjects. Response is expressed as percentage modulation, ΔR (power change relative to the prestimulus baseline). *Left column*: total response, containing phase-locked and non-phase-locked components. *Right column*: phase-locked response component only. This was isolated by averaging across trials in the time domain before transforming the data to the frequency domain.

only, the sliding window Fourier transform was applied after averaging across trials in the time domain.

We determined single-trial estimates of band-limited MEG activity in the following six frequency ranges: 4–8 Hz ("theta"), 8–12 Hz ("alpha"), 12–24 Hz ("beta"), 24–36 Hz ("high beta"), 36–56 Hz ("low gamma"), and 64–100 Hz ("high gamma"). Thus our analyses covered the entire frequency range from 4 to 100 Hz, with the exception of the range 60 ± 4 Hz, containing the phase-locked response to the LCD projector refresh (see RESULTS). The spectral estimates were computed for *1*) the prestimulus baseline interval (−0.5 s, stimulus onset) and *2*) the steady-state stimulus response after the initial onset transient (extending from 0.25 to 2 s after stimulus onset). The single-trial stimulus responses were then converted into units of percentage modulation according to *Eq. 1*, using the average baseline for each condition (see following text). To create time courses of MEG responses, we shifted a 500-ms window (step size: 50 ms) across the trial (0.5 s before stimulus onset to 2.5 s after stimulus offset) and computed spectral estimates for each time bin. We estimated the SE of all mean stimulus responses with a jackknife procedure (Efron and Tibshirani 1998).

IDENTIFICATION OF PERFORMANCE-RELATED MEG ACTIVITY. To analyze performance-related modulations of MEG activity we sorted the single-trial responses within each band according to the correctness of subjects' subsequent behavioral choice. To this end, we recombined single-trial responses across hits and correct rejects (correct) and across misses and false alarms (incorrect). We estimated the spectral MEG power during stimulus and baseline intervals separately for the correct and error conditions. Cortical population activity fluctuates strongly in the absence of sensory input (Arieli et al. 1996; Leopold et al. 2003). Such fluctuations of spontaneous activity may have a strong effect on the accuracy of subsequent stimulus processing (Linkenkaer-Hansen et al. 2004; Ress et al. 2000; Sapir et al. 2005). To minimize the contribution of potentially performance-related baseline fluctuations to our estimates of the stimulus-induced MEG activity, we normalized each single-trial response with the condition-wise (correct/error) average baseline power spectral density using *Eq. 1*. We could then analyze the difference in MEG activity between correct and incorrect behavioral choices independently for the "raw" band-limited MEG power spectral density during the baseline interval and the baseline-corrected stimulus-induced response. Comparing the raw MEG activity during stimulation between both behavioral conditions yielded qualitatively identical results.

We tested the association between MEG responses and subjects' behavior using a receiver operating characteristic (ROC) analysis (Green and Swets 1966). This analysis quantifies the overlap of single-trial MEG activity distributions for subjects' behavioral choices. The resulting index ranges between 0 and 1. An index of 0.5 implies that there is no discernible correlation between neural activity and behavioral response, whereas indices of 1 or 0 describe perfect correlations or anticorrelations, respectively. The index quantifies the accuracy with which an ideal observer can predict some binary aspect of the behavioral response (in this case: correct/error) from the neural activity during that trial. If prediction accuracy is at chance, the index is 0.5. Significant deviations from 0.5 in both directions imply that the behavioral performance is predictable from the neural activity parameter under study. We used a nonparametric permutation test (Efron and Tibshirani 1998) with 10^4 permutations to test each index for significant deviation from 0.5.

SOURCE RECONSTRUCTION: GENERAL PRINCIPLES. We used an adaptive spatial-filtering technique termed linear "beam forming" (Gross et al. 2001; Van Veen et al. 1997) for all source analyses subsequently described. That is, we applied frequency- and location-specific filters to the MEG data to estimate the local power spectral density in source space. More specifically, for each point of interest $\mathbf{r}$ in source space, we computed a frequency-specific filtering matrix $\mathbf{A}(\mathbf{r}, f)$ that passes band-limited activity from $\mathbf{r}$ with unit gain, while maximally suppressing the activity from all other sources. These constraints yield

$$\mathbf{A}(\mathbf{r},f)=[\mathbf{L}^T(\mathbf{r})\mathbf{C}(f)^{-1}\mathbf{L}(\mathbf{r})]^{-1}\mathbf{L}^T(\mathbf{r})\mathbf{C}(f)^{-1} \quad (2)$$

where the columns of $\mathbf{L}(\mathbf{r})$ contain the solution of the forward problem for two orthogonal tangential dipoles at location $\mathbf{r}$, and $\mathbf{C}$ denotes the complex cross-spectral–density matrix of the recorded MEG in the frequency range of interest (Gross et al. 2001). That is, the filter depends on the lead field (i.e., the mapping from source space to sensor space) and on the cross-spectral–density matrix of the recorded data. We estimated the cross-spectral–density matrix separately for the baseline (500 ms before stimulus onset) and motion viewing (250 ms to 2 s after stimulus onset) intervals, using the multitaper method. To compute the lead field for each individual sensor, we modeled the head as a set of multiple overlapping spheres, one per each sensor (Huang et al. 1999). This was based on the segmentation of the scalp in the structural MRI data set. We then computed the estimate of power spectral density $P(\mathbf{r}, f)$ according to

$$\mathrm{P}(\mathbf{r},f)=\lambda_1[\mathbf{A}(\mathbf{r},f)\mathbf{C}(f)\mathbf{A}^{*T}(\mathbf{r},f)] \quad (3)$$

where λ_1 denotes the largest singular value of the cross-spectrum estimates of the two dipoles (with fixed orientations). Thus λ_1 is the power of a dipole pointing into the dominant direction at location $\mathbf{r}$.

Downloaded from jn.physiology.org on July 27, 2007

We computed the estimate of local power spectral density $P(\mathbf{r}, f)$ separately for the prestimulus baseline and the steady-state response interval and then converted the source-level stimulus responses into units of percentage modulation using *Eq. 1*.

VOXELWISE ANALYSIS. To analyze the cortical distribution of the performance-related effect, we performed a voxelwise beam forming analysis to compute statistical parametric maps for the difference of sustained 12- to 24-Hz MEG activity between correct and incorrect choices. We divided the source space into a regular grid of 7.5 × 7.5 × 7.5-mm resolution covering the entire cerebral cortex. We computed the spatial distribution of MEG responses in the 12- to 24-Hz range for each run and behavioral condition (correct/error). We used a jackknifing procedure (Efron and Tibshirani 1998) to estimate the voxelwise means and SEs of these MEG response maps: We reconstructed n MEG response maps (where n is the number of trials for each condition), each map by leaving out one different trial in turn. We could then use the resulting ensemble of MEG response maps to compute the mean response and its SE at each location $\mathbf{r}$ for both behavioral conditions. These maps of response means and SEs were converted into t-maps testing the voxelwise difference between both conditions. These t-maps were converted into z-maps, linearly interpolated to a regular grid of 1-mm^3 resolution, pooled across runs, transformed to stereotactic standard space in BrainVoyager, and finally pooled across subjects. The spatial distribution of power spectral density depends on the cross-spectral–density matrix of the sensor data, which, in turn, contains at most $150^2 = 22{,}500$ independent real-valued numbers. Therefore we corrected all statistical maps with a factor of 22,500 for multiple comparisons (Bonferroni). Individual maps were thresholded at $P = 0.05$ (corrected). The group-average map was thresholded at $P = 10^{-3}$ (corrected).

REGION-OF-INTEREST ANALYSIS. We conducted a region-of-interest beam forming analysis of single-trial MEG responses to quantify the association between psychophysical performance and 12- to 24-Hz activity in three key stages of the dorsal visual pathway (Haxby and Ungerleider 1994): area MT+, the posterior intraparietal sulcus (pIPS), and the dorsolateral prefrontal cortex (dlPFC). We defined these regions of interest on each subject's structural MRI, based on a combination of anatomical and functional criteria independent of the data analyzed in the present study. MT+ was located in the junction of the ascending limb of the inferior temporal sulcus with its posterior continuation (Dumoulin et al. 2000). fMRI data from standard localizer protocols (e.g., Huk et al. 2002) were available for three of the four subjects. The functional definitions of MT+ obtained from these data sets were in close correspondence with the anatomical criteria. For pIPS, we identified the sharp transition from the deeper, but less truncated, posterior segment to the shallower, but more truncated, anterior segment of the human IPS (Donner et al. 2000). This transition was clearly discernible in all subjects. The pIPS location was placed in the middle of the posterior segment of the sulcus. The dlPFC location was placed at the anterior end of the posterior third of the medial frontal gyrus.

We estimated the single-trial MEG responses of each region of interest. We then analyzed their link to behavior in a number of different schemes. In the first scheme, we collapsed the region of interest responses across hemispheres. We sorted (in increasing order) the trials according to the magnitude of these pooled responses. We grouped the data into bins of equal number of trials, based on the MEG response. Each trial was further labeled according to its signal detection category (i.e., correct reject, false alarm, miss, or hit). We could thus compute the average MEG response and d' for each bin, where d' is a bias-free measure of detection performance derived from the proportions of hits and false alarms (Green and Swets 1966). We could then test the linear regression between the region's MEG response and detection performance. To control for the effect of bin size, we repeated the analysis with several different bin sizes, from 50 to 400 trials per bin, in steps of 10. We evaluated the resulting linear fit at the 2.5th and the 97.5th percentiles of the measured MEG responses. We used the difference between the two resulting d' values as a measure for the amount of performance fluctuations explained by the MEG responses. That is, performance changes were expressed in terms of $\Delta d'$ (i.e., in SD units). In addition, we converted both d' values into units of percentage correct, according to

$$P_{\max}(correct) = F(0.5 \times d') \times 100\% \quad (4)$$

where F denotes the normal cumulative distribution function. $P_{\max}(correct)$ equals the maximal percentage of correct responses, achievable in the absence of bias, given the measured sensitivity of the observer (Green and Swets 1966). The difference between the upper and lower values, $\Delta P_{\max}(correct)$, is a complementary measure of performance changes explained by the MEG responses.

We were also interested in whether the stimulus-induced response was correlated with the strength of the performance-related modulation in the regions of interest. To analyze this correlation, we sorted log-transformed single-trial responses in ascending order and grouped them into bins of 50 trials. Each bin contained a number of correct and error trials. We calculated two variables for each bin: the mean overall response and the *difference* between the mean response on correct and error trials (i.e., the behavioral modulation of the response). We then tested the linear regression between the two variables, again varying the bin size across several steps.

In a final scheme, we again used ROC analysis (Green and Swets 1966), now at the cortical source level. In each region of interest, we compared the band-limited MEG response distributions corresponding to subjects' "yes" and "no" choices, separately for both stimulus conditions (i.e., target present and target absent). The predictive indices in this analysis describe the link between neural activity and subjects' "yes" and "no" choices, rather than the correctness of response. We therefore labeled them "choice probabilities" (CPs), in conformity with previous single-unit studies (e.g., Britten et al. 1996; Kim and Shadlen 1999; Shadlen and Newsome 2001; Uka and DeAngelis 2004; Williams et al. 2003), Again, we tested the ROC indices for significant deviation from 0.5 with a permutation test (10^4 permutations).

CONTROL ANALYSIS. Simulation studies suggest that highly correlated sources (between 0.95 and 1) may be mislocalized by the beam-forming technique (Van Veen et al. 1997). These errors are twofold: closely spaced (~3 mm) sources tend to merge, whereas distant sources (~12 mm) cancel each other out. Correlations of <0.5 are tolerable (Gross et al. 2001; Van Veen et al. 1997). Cortical coherence is commonly <0.5 in all frequency bands for distances >5 mm (Leopold et al. 2003). This is an order of magnitude below the spatial scale relevant to the anatomical hypotheses addressed in the present study. We are therefore confident that source correlations do not affect our conclusions regarding response differences between cortical regions several centimeters apart from each other. Furthermore, our previous beam forming analyses of the cortical distribution of MEG responses to gratings and random-dot patterns yielded plausible results (e.g., Hoogenboom et al. 2005; Siegel et al. 2007). We aimed to establish this also for the present data set. High gamma band activity in primate early visual cortex (V1/V2) is strongly modulated by high-contrast stimuli (Henrie and Shapley 2005; Hoogenboom et al. 2005; Siegel et al. 2007). We therefore reconstructed the cortical distribution of the high gamma band (64–100 Hz) response to the random-dot patterns (averaged across all conditions). We then tested the voxelwise difference of the mean response from zero (using jackknife SEs) and generated statistical z-maps for this difference, as described earlier for the analysis of performance-related activity. In all four subjects, the global maximum of the response was localized in close vicinity to the calcarine sulcus, that is, in early visual cortex

Downloaded from jn.physiology.org on July 27, 2007

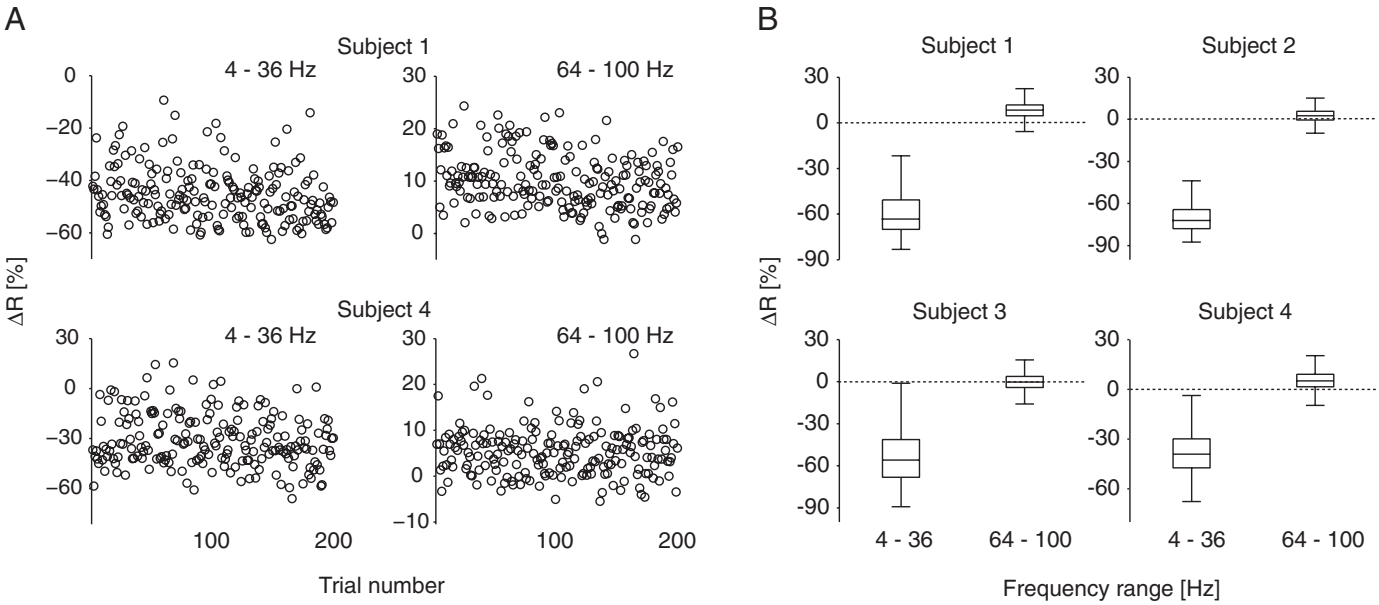

FIG. 3. MEG responses during motion viewing fluctuate strongly from trial to trial. *A*: single-trial responses in the low- (4- to 36-Hz) and high- (64- to 100-Hz) frequency ranges for a representative sequence of 200 trials in 2 exemplary subjects. Responses are calculated for the steady-state interval (0.25–2 s after stimulus onset). *B*: box plots representing the distributions of the complete set of single-trial responses (same frequency ranges and time interval as in *A*). Lower and upper bounds of the boxes indicate the lower and upper quartiles, respectively. Horizontal lines within the boxes represent the medians. Vertical lines above and below the boxes show the overall range of the data, excluding outliers. Maximum length of these lines corresponds to 1.5 times the interquartile range (an estimator of the spread of the data). Responses are averages across the sensors of interest shown in Fig. 2.

(Supplemental Fig. 1).[1] This finding lends support to the source reconstructions of the more subtle performance-related effect described in RESULTS.

RESULTS

Each trial began with the presentation of a fixation cross for a variable baseline interval followed by the presentation of a dynamic random-dot pattern (Fig. 1). On one half of the trials, a target pattern was presented that contained a small proportion of dots moving coherently in one direction. On the other half of the trials, a noise pattern was presented that contained no coherent motion. Subjects formed a decision about the presence or absence of the target. The strength (coherence) of the target motion was adjusted individually such that each subject performed at roughly 71% correct ($d' \sim 1.1$). We collected MEG data during several thousands (3,600–6,000) trials per subject.

MEG responses to dynamic random-dot patterns

We first characterized the time course and spectral signature of MEG responses to the moving random-dot patterns at the level of MEG sensors, averaging responses across a fixed set of 20 posterior sensors consistently displaying a strong stimulus response (Fig. 2). In particular, the dynamic random dot patterns induced a steady-state response that followed a transient response, began at about 250 ms after stimulus onset, and was sustained as long as the stimulus remained on the screen. This steady-state response had a characteristic spectral profile: MEG power decreased at frequencies ranging from about 4 to 50 Hz and increased at frequencies between about 60 and 150 Hz. This closely resembles the visual MEG response obtained in previous studies for higher levels of motion strength (Siegel et al. 2007) and high-contrast moving gratings (Hoogenboom et al. 2005). The narrow-band power increase around 60 Hz reflects an entrainment to the refresh rate of the LCD projector (Williams et al. 2004). This was confirmed by its persistence in the phase-locked ("evoked") response component shown in the *right column* of Fig. 2. At all other frequencies, the strong steady-state response evident in the *left column* was absent in the phase-locked response component in the *right column*. Thus apart from 60 Hz, the steady-state response reflects non-phase-locked ("induced") perturbations of ongoing cortical population activity (Pfurtscheller and Lopes da Silva 1999; Tallon-Baudry and Bertrand 1999). The low- and high-frequency components of the steady-state response both fluctuated strongly from trial to trial, as evident in exemplary trial sequences shown in Fig. 3*A*. In all four subjects, the variability of both response components (measured by the interquartile range) was of a magnitude similar to that of the median response (Fig. 3*B*).

Covariation of MEG activity and behavioral detection performance

We proceeded by testing whether, and if so, in which frequency range these response fluctuations predicted subjects' psychophysical performance. We estimated the single-trial responses of the same sensor group in six frequency bands covering the range of the steady-state response and sorted these according to the correctness of subjects' subsequent choices (Fig. 4, *left column*). To minimize the contribution of potential performance-related prestimulus activity, we normalized the stimulus responses for correct and incorrect trials with the condition-wise (correct/error) baseline. MEG activity in the 12- to 24-Hz (low beta) range was larger before correct than

[1] The online version of this article contains supplemental data.

Downloaded from jn.physiology.org on July 27, 2007

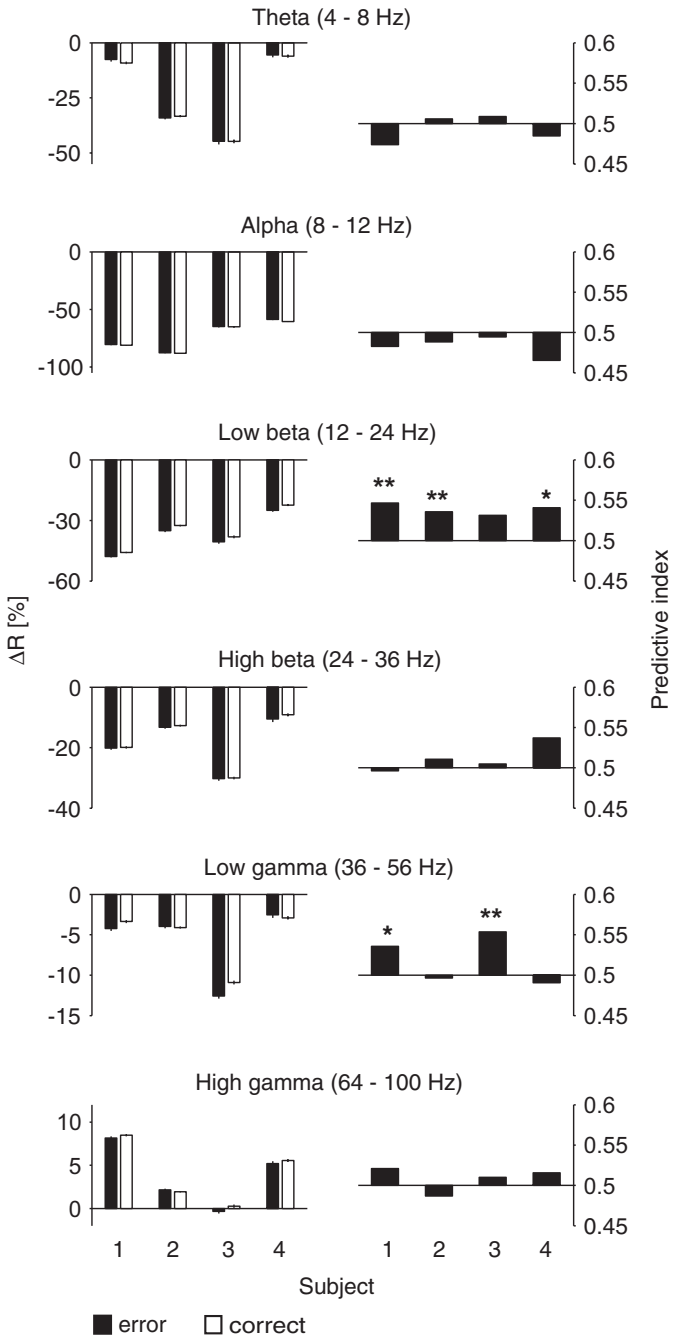

FIG. 4. MEG activity during motion viewing predicts behavioral detection performance. *Left column*: average band-limited steady-state MEG responses on correct and incorrect trials (0.25–2 s after stimulus onset). Rows correspond to six frequency bands covering the steady-state MEG response. Error bars indicate jackknife SE. *Right column*: receiver operating characteristic (ROC) indices quantifying the predictability of correct behavioral choices from the band-limited MEG responses. Asterisks indicate the significance of their deviation from 0.5, derived from a permutation test (*$P < 0.05$; **$P < 0.01$; corrected for multiple comparisons). Responses are means across the sensors of interest shown in Fig. 2.

before incorrect choices in all four subjects. More specifically, there was consistently less stimulus-induced suppression of MEG activity in the 12- to 24-Hz range before correct than before incorrect choices. The same was true for the 36- to 56-Hz (low gamma) range in two of the subjects. Note that the performance-related enhancement of MEG activity was confined to a relatively narrow frequency range in all subjects, whereas the suppression by the visual stimulus consistently spanned the entire range from about 4 to 50 Hz.

We used ROC analysis (see METHODS) to compute a predictive index that quantifies the association between MEG activity and behavior (Fig. 4, *right column*). A predictive index significantly different from 0.5 (chance level) indicates that the behavior can be predicted from the MEG responses on single trials. Specifically, an index >0.5 indicates that MEG responses tend to be larger before correct than before incorrect behavioral choices. For the 12- to 24-Hz range, prediction accuracy was above chance level in all four individuals (0.55, 0.54, 0.53, and 0.54). The average index (±SD) across subjects was 0.54 ± 0.007. The deviation from chance level was (highly) significant in three subjects and showed a trend toward significance in the fourth. For the 36- to 56-Hz range, prediction accuracy was significantly above chance in two subjects and averaged to 0.52 ± 0.035 across subjects. All other frequency ranges did not display a consistent relationship with behavior. In sum, the 12- to 24-Hz frequency range had the maximum average predictive power for correct behavioral reports (i.e., maximum average ROC index) and the maximum number of significant individual ROC indices. We therefore focused on this frequency range in our subsequent analyses.

The previous analysis did not reveal when during the trial the predictive activity evolved. Cortical activity fluctuates strongly in the absence of sensory stimulation (Arieli et al. 1996; Leopold et al. 2003). Such fluctuations of spontaneous cortical activity may be tightly correlated with the accuracy of subsequent stimulus processing (Linkenkaer-Hansen et al. 2004; Ress et al. 2000; Sapir et al. 2005). We wondered whether such a performance-related modulation of prestimulus MEG activity was evident in the present data. We compared the raw band-limited MEG power of the same sensor group as in the previous analysis during the 500 ms preceding stimulus onset between correct and error conditions. Surprisingly, significant prediction of correct choices was *not* possible based on the prestimulus MEG activity in any of these six frequency bands in any subject. The average ROC indices (±SD) for each band were as follows: 4–8 Hz: 0.50 ± 0.003; 8–12 Hz: 0.50 ± 0.007; 12–24 Hz: 0.50 ± 0.007; 24–36 Hz: 0.50 ± 0.006; 36–56 Hz: 0.51 ± 0.004; 64–100 Hz: 0.50 ± 0.012. Specifically, the individual ROC indices (*P*-values) in the 12- to 24-Hz ranged from 0.48 to 0.51 (0.11 to 0.76, uncorrected). Note that the lengths of the analysis windows differed for the baseline and stimulus intervals (500 vs. 1,750 ms), which prohibits direct quantitative comparisons between the corresponding ROC indices. Furthermore, the analysis of the baseline interval was based on raw MEG power, whereas the analysis of the stimulus interval was based on normalized responses. Nevertheless, the present result suggests that the effect of prestimulus activity on behavioral outcome was negligible. In addition, the lack of a baseline effect suggests that the performance-predictive activity observed during motion viewing is independent of the response normalization procedure.

We next analyzed the time course of 12- to 24-Hz activity in more detail by sliding a 500-ms window across the entire trial. Figure 5*A* shows the time courses for the *raw* MEG power, allowing for a direct comparison between baseline and stimulus intervals. Figure 5*B* shows the *relative* MEG responses, after normalization with the condition-wise baseline, allowing for a direct comparison with the previous analysis of the

Downloaded from jn.physiology.org on July 27, 2007

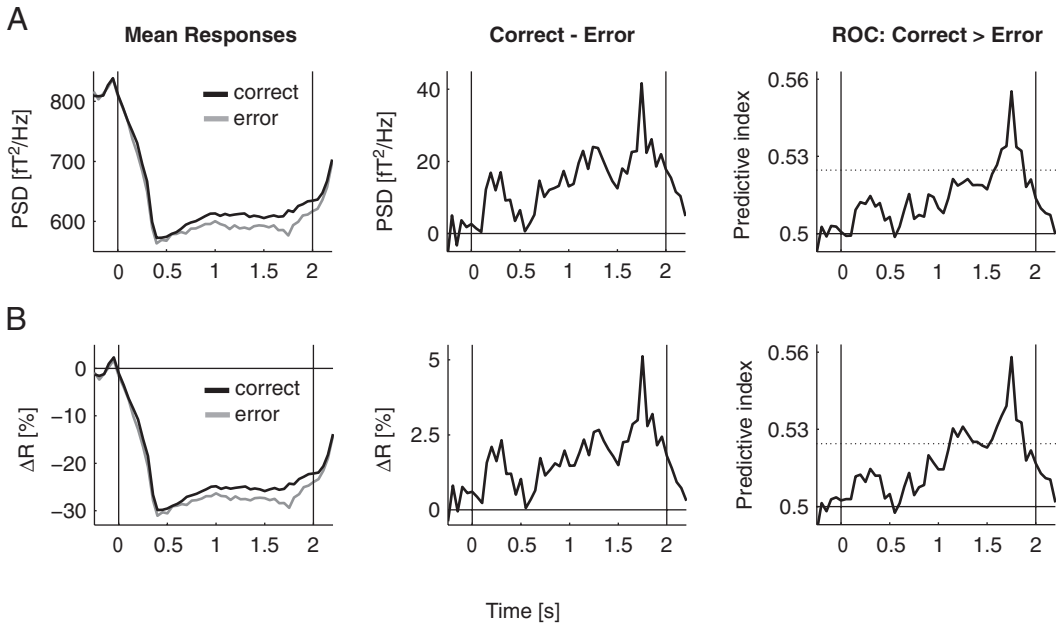

FIG. 5. Performance-predictive MEG activity builds up slowly during motion viewing. *Left*: group average time course of 12- to 24-Hz MEG responses for correct (black line) and incorrect (gray line) conditions. *Middle*: time course of the response difference between these behavioral conditions. *Right*: time course of the ROC index corresponding to the mean responses shown on the *left* (correct vs. error). Dotted line indicates the significance level ($P < 0.05$, permutation test). *A*: time courses of raw MEG power spectral density (PSD) and of the ROC index derived from the distributions of single-trial responses of raw PSD for correct and incorrect trials. *B*: time courses of stimulus-induced modulation (ΔR) and of the corresponding ROC index. Time courses are averaged across the sensor group shown in Fig. 2. Note the similarity between corresponding time courses in *A* and *B*, suggesting that the response normalization did not affect the results.

steady-state stimulus response interval. The time courses in Fig. 5, *A* and *B* are qualitatively identical, again suggesting that the performance-predictive effect is independent of the response normalization procedure. The raw MEG power was virtually identical before stimulus onset on correct and error conditions (Fig. 5*A*, *left*), reflecting the absence of performance-related baseline activity reported earlier. During motion viewing, 12- to 24-Hz responses on correct and error conditions began to diverge immediately after the initial negative transient and remained separated until stimulus offset (Fig. 5, *left*). In addition, the time courses of the response difference and the ROC index revealed a continuous increase throughout motion viewing until reaching a (highly significant) maximum shortly before stimulus offset (Fig. 5, *middle* and *right*). Thus the predictive activity built up slowly after stimulus onset, implying that 12- to 24-Hz activity during motion viewing is more strongly correlated with behavioral outcome later than earlier in the time. This buildup suggests that the process underlying the correlation either operates on a relatively fast (subsecond) timescale, or that it involves leaky temporal integration of sensory evidence (Cook and Maunsell 2002; Gold and Shadlen 2001), or both. It is important to emphasize that the performance-related MEG activity is specifically linked to the stimulus interval. This is in sharp contrast to the slow (multi-minute to minute) correlation between the ongoing EEG power and auditory detection performance observed in previous studies (e.g., Makeig and Inlow 1993). Furthermore, the sustained difference between correct and error conditions throughout the interval of the steady-state response supports our earlier choice of the analysis window (0.25–2 s after stimulus onset). We used the same window for all subsequent analyses at the source level.

Cortical distribution of performance-predictive 12- to 24-Hz activity

To characterize the cortical distribution of performance-predictive MEG activity we used spatial filtering to project the stimulus-induced steady-state activity in the 12- to 24-Hz range from the sensor space to the source space (see METHODS). We computed statistical maps for the differential activity before correct and incorrect behavioral responses. Local maxima of these maps were bilaterally located in the posterior parietal and dorsolateral prefrontal cortex both in the group average (Fig. 6) and in the majority of individual subjects (Table 1). In particular, the performance-related effect was expressed in and around the right posterior intraparietal sulcus in all four subjects. The effect was also expressed in the left hemisphere in this parietal region in two subjects. Local maxima were present bilaterally in the dorsolateral prefrontal cortex in all four subjects. However, their locations varied more strongly with respect to anatomical landmarks (the medial frontal gyrus and superior frontal sulcus) and the Talairach coordinate system, presumably reflecting larger intersubject variability in this cortical region. Further performance-predictive effects in the 12- to 24-Hz range were located in several regions involved in attention and detection (Corbetta and Shulman 2002) and in visual motion processing (Braddick et al. 2000; Rees et al. 2000): the temporoparietal junction (in the posterior part of superior temporal gyrus), the left inferior temporal and the fusiform gyrus, and an occipitotemporal region corresponding to the anatomical landmarks of MT+: the junction of the inferior temporal sulcus and its posterior continuation (Dumoulin et al. 2000; Huk et al. 2002). In sum, performance-related 12- to 24-Hz activity was widely distributed across motion-sensitive visual cortical areas, but it clearly predominated in two asso-

Downloaded from jn.physiology.org on July 27, 2007

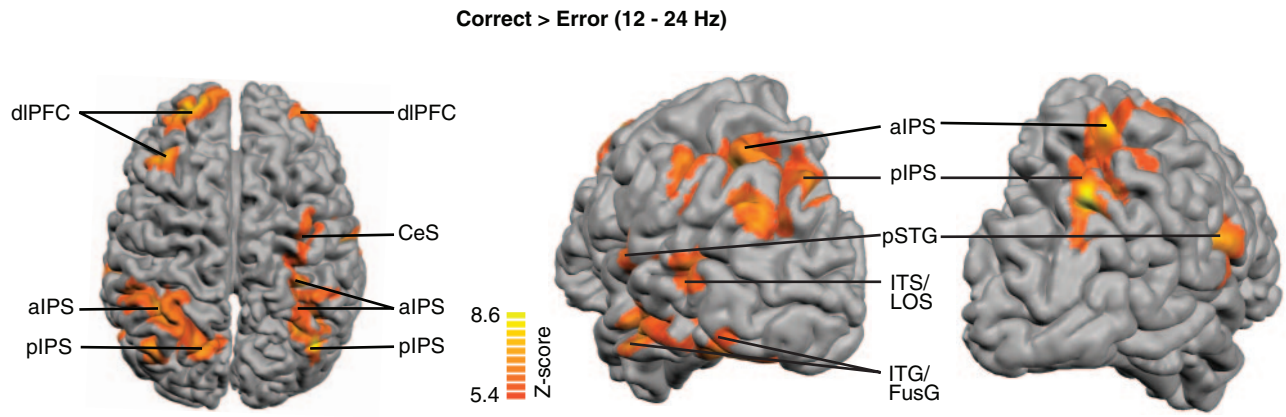

FIG. 6. Performance-predictive MEG activity is expressed in the dorsal visual pathway. The group-average statistical z-map for the comparison between steady-state 12- to 24-Hz activity (0.25–2 s after stimulus onset) before correct and incorrect choices is superimposed onto a reconstructed cortical surface of one subject. Map is thresholded at $P = 10^{-3}$ (corrected for multiple comparisons). *Left*: dorsal view (frontal pole at the *top*). *Right*: posterolateral view. Abbreviations: dlPFC, dorsolateral prefrontal cortex; CeS, central sulcus; a/pIPS, anterior/posterior intraparietal sulcus; ITS, inferior temporal sulcus; LOS, lateral occipital sulcus; pSTG, posterior superior temporal gyrus; ITG, inferior temporal gyrus; FusG, fusiform gyrus.

ciation areas implicated in visual attention and detection processes (Corbetta and Shulman 2002): posterior intraparietal sulcus and the dorsolateral prefrontal cortex.

We next quantified the link between the MEG activity in these two regions and detection performance in more detail. We defined locations of interest within both regions based on anatomical criteria (METHODS) and labeled these pIPS and dlPFC. We estimated their single-trial MEG responses and collapsed them across the left and right hemispheres. We sorted the trials according to the magnitude of the response in both regions of interest and binned the trials, based on the response amplitude. We then computed, for each bin, a mean MEG response and behavioral performance, expressed in d' (i.e., in SD units). The linear regression between MEG activity in the 12- to 24-Hz range and d' showed highly significant positive slopes in each subject in both regions of interest (Fig. 7). We varied the bin size from 50 to 400 in steps of 10 and found that the effect was significant for all bin sizes. The average across subjects was also highly significant for both regions, again irrespective of the bin size. We then used these linear fits to gain a quantitative description of the association between the fluctuations of frontoparietal activity and behavioral performance. For both regions, increases of 12- to 24-Hz activity from the 2.5th to the 97.5th percentile of the single-trial responses explained, on average, increases of performance by roughly 17% percentage correct ($d' = 1.1$). The sensor-level analysis also revealed performance-predictive activity in the 36- to 56-Hz range, and thus we also repeated the analysis for this frequency range. The results in dlPFC were inconsistent and insignificant on average. However, the correlation between 36- and 56-Hz activity and d' was significant in the grand average and in two individuals in pIPS (Supplemental Fig. 2). To sum up, 12- to 24-Hz MEG activity in pIPS and dlPFC accounted for a substantial amount of the fluctuations of subjects' detection performance near threshold.

TABLE 1. *Cortical regions with performance-related 12- to 24-Hz MEG activity during motion viewing*

Region	Brodman Area	Hemisphere	Talairach Coordinates (±SD)			*n*
			X	Y	Z	
Frontal						
MFG/SFS	46/9	L	−30 (10)	22 (32)	42 (13)	4
	46/9	R	26 (14)	30 (23)	41 (25)	4
Ventral PreCeS	6/9	R	47 (8)	1 (6)	41 (13)	2
CeS	4	R	37 (12)	−20 (5)	54 (2)	2
Parietal						
Anterior IPS	7	L	−45 (6)	−53 (2)	44 (7)	2
	7	R	37 (6)	−50 (2)	56 (6)	2
Posterior IPS	7	L	−24 (8)	−78 (8)	52 (8)	2
	7	R	28 (10)	−76 (7)	41 (14)	4
Temporal						
Posterior STG	22/39	L	−57 (0)	−45 (12)	37 (3)	2
	22/39	R	59 (10)	−31 (18)	20 (6)	2
Lateral FusG/ITG	37/19	L	−48 (8)	−64 (11)	−16 (12)	3
	37/19	R	52 (10)	−56 (31)	−21 (6)	2
Occipital						
Pericalcarine	17/18		−3 (12)	−97 (8)	−2 (5)	3

X, Y, and Z are average Talairach coordinates (±SD) of local maxima of individual z-maps for the comparison of sustained 12- to 24-Hz responses (0.25–2 s after stimulus onset) before correct versus incorrect judgments; *n* is the number of subjects with the respective local maximum. Only regions significant at $P < 0.05$ (corrected) in at least two subjects are listed. Abbreviations: MFG, medial frontal gyrus; PreCeS, precentral gyrus; CeS, central gyrus; IPS, intraparietal sulcus; STG, superior temporal gyrus; ITG, inferior temporal gyrus; FusG, fusiform gyrus.

Downloaded from jn.physiology.org on July 27, 2007

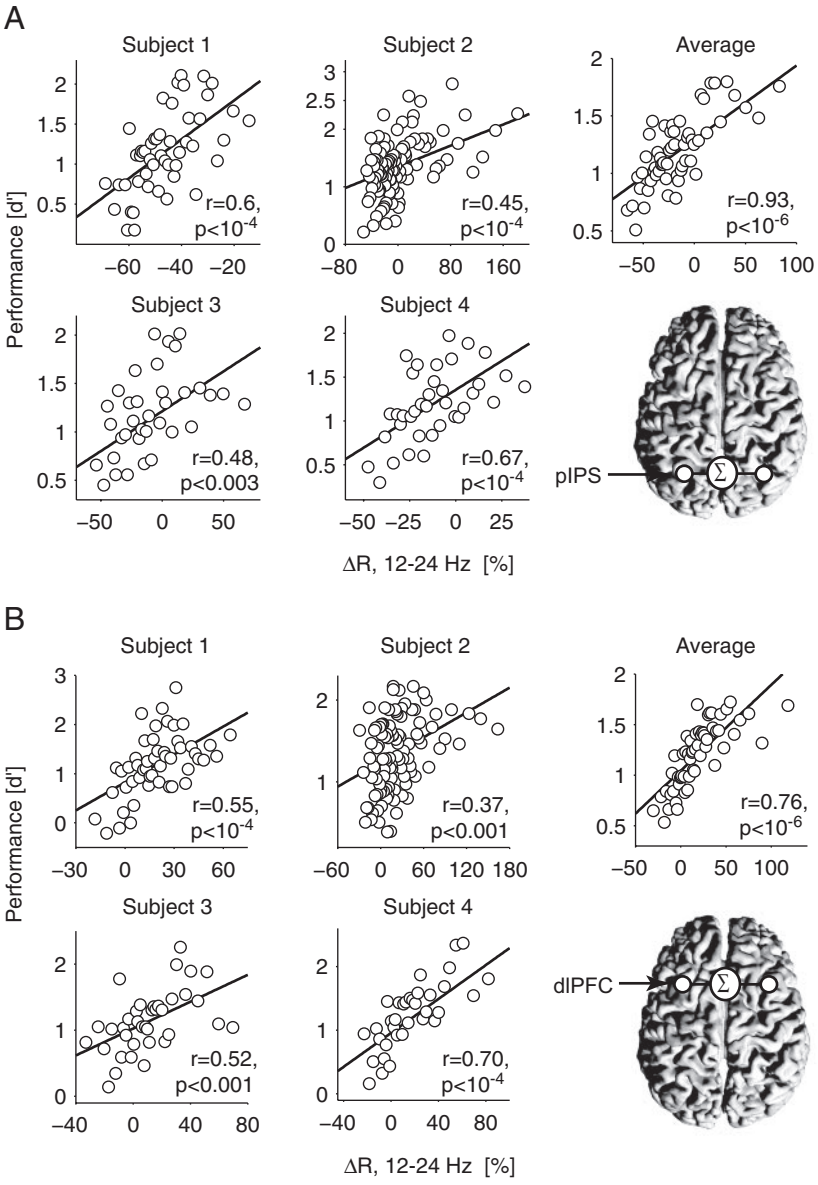

FIG. 7. MEG activity in parietal and prefrontal cortex explains a large amount of behavioral performance fluctuations. *A*: linear regression between the steady-state 12- to 24-Hz response ΔR (0.25–2 s after stimulus onset) in pIPS and d'. Bin size is 50 trials for the individual subjects and 200 trials for the grand average. *B*: same as in *A*, for dlPFC. *Insets*: regions of interest are depicted on the reconstruction of one subject's cortical surface. Average across both hemispheres has been taken as the neural response variable in the correlation analyses.

The different spectral signatures of the stimulus-induced suppression and of the performance-related modulation of 12- to 24-Hz MEG activity observed at the scalp suggest that the two reflect different processes. We addressed this issue more directly by correlating both variables, separately for both regions of interest. To this end, we again binned trials by the response magnitude of each region and computed for each bin the mean overall response and the difference between the mean responses on correct and error trials (i.e., the performance-related modulation). We then tested the linear correlation between the overall response and the performance-related modulation. In both regions, this correlation did not attain significance in any subject. Average correlation coefficients were 0.016 for pIPS and 0.003 for dlPFC. The corresponding *P*-values ranged between 0.41 and 0.97. In other words, the strength of the stimulus responses in both parietal and prefrontal cortex did not covary with the strength of their performance-related modulation. This absence of correlation strongly supports the hypothesis of independent underlying processes.

Role of large-scale 12- to 24-Hz activity in perceptual decision making

A final set of analyses aimed at determining whether the MEG activity in key stages of the dorsal pathway reflected the *content* or the *accuracy* of subjects' choices. To address this issue we compared single-trial responses in the 12- to 24-Hz range between "yes" and "no" choices, separately for the target-present and target-absent conditions. That is, we separately compared hits with misses and false alarms with correct rejects. Because the predictive index derived from this ROC analysis describes the link between neural activity and perceptual choice, we labeled it "choice probability" (CP). If MEG activity predicts the content of the observer's perceptual reports, then the magnitude of responses before "yes" choices should be larger than that before "no" choices in both target-absent and target-present conditions. Correspondingly, CP should deviate from 0.5 in the same direction in target-absent and -present conditions (Fig. 8*A*, *left*). If MEG activity instead reflects the observer's accuracy, then the ranking of responses

Downloaded from jn.physiology.org on July 27, 2007

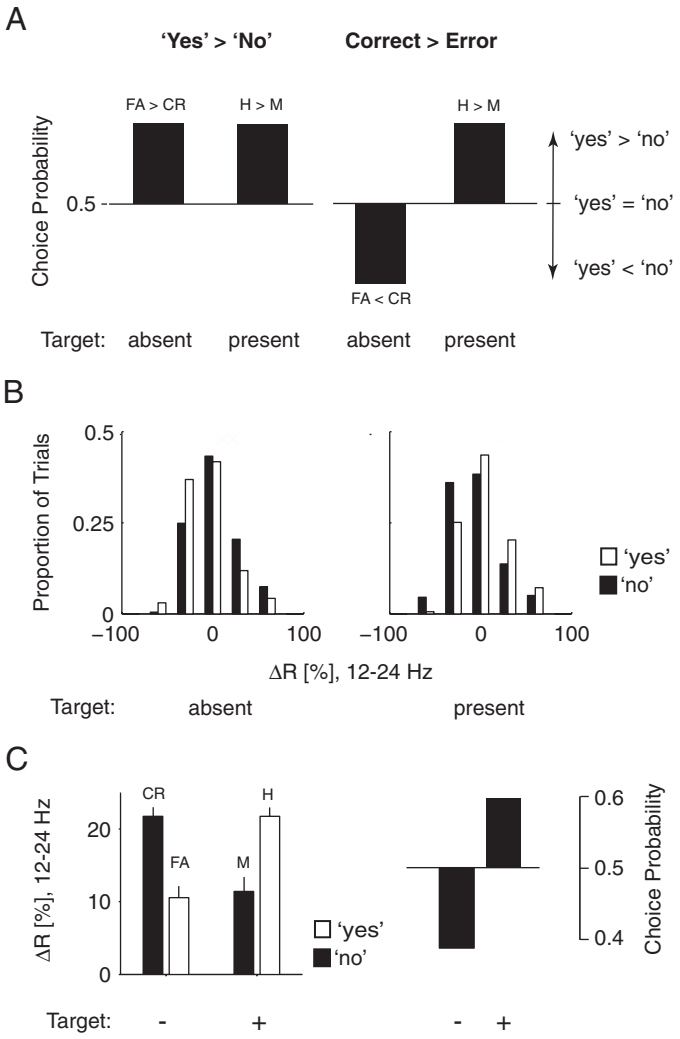

FIG. 8. Choice probability (CP) analysis of target-absent and -present trials pinpoints the functional role of performance-predictive MEG activity. Upward deviation of CP from 0.5 (chance level) indicates higher MEG activity before "yes" than before "no" choices (vice versa for downward). *A*: predicted pattern of CPs in target-absent and -present conditions for two different functions of a neural activity parameter in the perceptual choice. *Left*: activity tends to be larger before "yes" than before "no" choices, irrespective of their correctness. *Right*: activity tends to be larger before correct than before incorrect choices, irrespective of their content. *B*: exemplary distributions of 12- to 24-Hz responses, ΔR (0.25–2 s after stimulus onset) on target-absent and target-present conditions (dlPFC, subject 4). Distributions are sorted according to "yes"/"no" choice. Responses tend to be larger before "no" than before "yes" choices for target-absent trials and vice versa for target-present trials. *C*, *left*: mean responses, ΔR, for each stimulus/choice combination (error bars: jackknife SE). *Right*: CPs for target- present and -absent conditions. Prefrontal 12- to 24-Hz activity predicts the accuracy, and not the content, of the subject's upcoming choices. Abbreviations: CR, correct rejects; FA, false alarms; M, misses; H, hits; −, target-absent condition; +, target-present condition.

before "yes" and "no" reports should reverse in sign for target-absent and -present conditions. Correspondingly, CP should deviate from 0.5 in opposite directions (Fig. 8*A*, *right*). An example of this analysis is shown in Fig. 8, *B* and *C* for the dlPFC of one subject (subject 4). The 12- to 24-Hz responses in this region tended to be larger before correct than before incorrect choices, irrespective of the content of the perceptual report. This is evident in the response distributions for "yes" and "no" choices on target-absent and target-present conditions (Fig. 8*B*) as well as in the corresponding response means and CPs (Fig. 8*C*). Specifically, CP deviated from 0.5 in opposite directions in target-absent and -present conditions. Thus 12- to 24-Hz activity in this region predicts the accuracy, and not the content, of the subject's upcoming perceptual reports.

Areas dlPFC, pIPS, and MT+ all showed the same qualitative pattern of choice-related modulation: CP consistently deviated from 0.5 in opposite directions in target-absent and -present conditions (Fig. 9). In the target-present condition, these deviations in all three areas were (highly) significant in each subject. In the target-absent condition, they were (highly) significant in one subject in MT+, in three subjects in pIPS, and in two subjects in dlPFC. Most of the remaining tests approached significance. The average CPs were 0.46, 0.44, and 0.45 for target-absent stimuli and 0.56, 0.57, and 0.60 for target-present stimuli in MT+, pIPS, and dlPFC, respectively. Thus in each area, there was a bias toward stronger choice-related modulation in the target-present condition, presumably reflecting an additional signal associated with hits (Corbetta and Shulman 2002; Shulman et al. 2001). However, the opposite pattern of CP in the target-absent condition clearly indicates that the 12- to 24-Hz activity in none of the three areas was generally larger before, and thus specifically associated with, "yes" choices. The 12- to 24-Hz activity in the dorsal pathway reflects the accuracy, rather than content, of visual-detection decisions.

Note that the 12- to 24-Hz activity was enhanced in the dlPFC, as opposed to suppression in MT+ and pIPS. Thus the sign of the stimulus response changed between posterior and anterior regions of the dorsal pathway, whereas the sign of the performance-related response *difference* in the 12- to 24-Hz range remained constant. This dissociation between stimulus-induced and performance-related MEG activity adds strongly to our earlier conclusion, that the two reflect independent processes. Also note that various nonneural (instrumental, environmental, and physiological) noise sources and the activity of non-task-related neuronal populations contribute to the measured MEG response distributions. Therefore the CPs reported here should be considered only a lower bound of the "true" association between the 12- and 24-Hz activity in each region and behavioral choice.

Having established a trial-to-trial covariation between MEG responses in the dorsal pathway and subjects' detection accuracy, we went on to pinpoint the source of this covariation. In principle, variations in the dynamic stimuli could cause such an effect, if they were correlated with both the strength of the MEG response and behavioral choice. Recall that in the target-absent condition, subjects viewed exactly the same noise stimuli on each trial, excluding this possibility. On target-present trials, however, targets moved either upward or downward, although subjects judged only the presence or absence of coherent motion. Psychophysical detectability of, and MEG responses to, these two different moving patterns may have differed slightly, which may have caused the observed correlation. We therefore repeated the analysis for the target-present condition after splitting up the trials according to motion direction. The pattern of CP indicated higher 12- to 24-Hz activity before hits than before misses, irrespective of motion direction (Table 2). Significance was reduced in comparison to the previous analysis, reflecting the reduced statistical power. However, CPs tended to be >0.5 in each region and in fact

Downloaded from jn.physiology.org on July 27, 2007

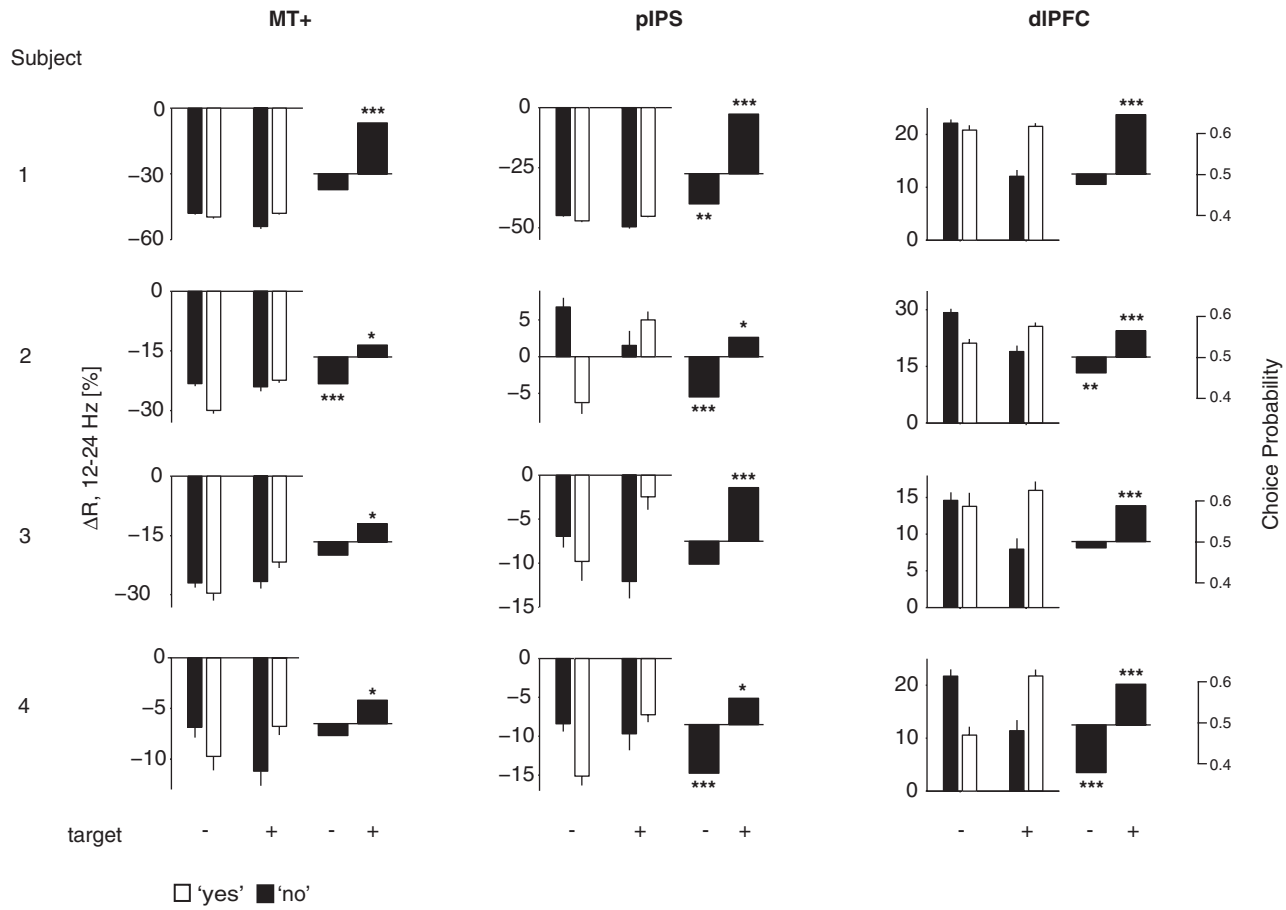

FIG. 9. Activity (12–24 Hz) in the dorsal visual pathway predicts the accuracy of perceptual choice. Choice-related 12- to 24-Hz MEG activity is depicted for the steady-state response (0.25–2 s from stimulus onset) in areas MT+, pIPS, and dlPFC. Format is as in Fig. 8*C*. For each region of interest, the *left column* shows mean responses, ΔR, sorted according to stimulus and choice (error bars: jackknife SE). *Right column*: corresponding CPs for target-absent and -present conditions (*$P < 0.05$, **$P < 0.01$, ***$P < 10^{-3}$, permutation test). Note that all CPs deviate in opposite directions from 0.5 in target-absent and -present conditions. Abbreviations: CR, correct rejects; FA, false alarms; M, misses; H, hits; −, target-absent condition; +, target-present condition; MT+, human visual motion-complex V5/MT+; pIPS, posterior intraparietal sulcus; dlPFC, dorsolateral prefrontal cortex.

larger than that in the previous analysis, suggesting that stimulus-induced variability may have camouflaged a part of the choice-related modulation in the previous analysis. Average CPs were 0.58 (upward) and 0.55 (downward) in MT+, 0.56 (upward) and 0.59 (downward) in pIPS, and 0.62 (upward and downward) in dlPFC. Thus also on target-present trials, the covariation between MEG responses and behavioral choice did not depend on the variation of motion direction. This implies that the covariation between MEG activity and perceptual choice on both target-present and -absent trials was *not* driven by the stimulus, but originated from sources inside the brain.

fMRI responses (Rees et al. 2000) and high gamma band MEG activity (Siegel et al. 2007) in human motion-sensitive visual areas, including MT+, increase monotonically with motion strength. One might therefore expect that MEG activity in the gamma band correlates with subjects' motion present/absent perception. Note that a "pure" correlation with choice content (false alarms > correct rejects and hits > misses, with equal differences between choice categories) might have obscured an effect in our previous analysis of correct versus error trials. We therefore repeated the CP analysis for the 64- to 100-Hz range. We did not find a content-related pattern of CP

TABLE 2. *Choice probabilities based on 12- to 24-Hz MEG activity for upward and downward motion stimuli*

	MT+				pIPS				dlPFC			
Subject	1	2	3	4	1	2	3	4	1	2	3	4
Up												
CP	**0.63**	0.52	0.52	**0.64**	**0.64**	0.51	0.46	**0.63**	**0.60**	**0.59**	**0.64**	**0.66**
P	$<10^{-3}$	0.29	0.62	$<10^{-3}$	$<10^{-3}$	0.75	0.24	$<10^{-3}$	$<10^{-3}$	$<10^{-3}$	$<10^{-3}$	$<10^{-3}$
Down												
CP	**0.65**	0.48	0.51	0.56	**0.58**	0.52	**0.58**	**0.66**	**0.67**	0.54	**0.63**	**0.64**
P	$<10^{-3}$	0.40	0.82	0.14	0.04	0.41	0.04	$<10^{-3}$	$<10^{-3}$	0.07	$<10^{-2}$	$<10^{-3}$

Values are choice probabilities (CPs) and the corresponding null hypothesis probabilities (*P*-values) for upward and downward motion stimuli (see main text for details). CPs > 0.5 with values of $P < 0.05$ are in bold.

Downloaded from jn.physiology.org on July 27, 2007

TABLE 3. *Choice probabilities based on 64- to 100-Hz MEG activity for noise and target stimuli*

	MT+				pIPS				dIPFC			
Subject	1	2	3	4	1	2	3	4	1	2	3	4
Noise												
CP	0.51	0.49	0.53	0.54	0.46	**0.47**	**0.46**	**0.55**	0.52	0.51	0.52	0.51
P	0.70	0.58	0.14	0.10	0.07	0.04	0.01	0.02	0.30	0.43	0.30	0.77
Target												
CP	0.52	**0.42**	**0.44**	0.49	**0.57**	**0.53**	**0.58**	0.47	**0.45**	0.47	0.48	**0.43**
P	0.43	$<10^{-3}$	0.02	0.14	0.01	0.02	$<10^{-2}$	0.10	0.04	0.43	0.34	$<10^{-3}$

Values are choice probabilities (CPs) and the corresponding null hypothesis probabilities (*P*-values) for target-absent (noise) and target-present stimuli (see main text for details). CPs with values of $P < 0.05$ are in bold.

in any of the three regions of interest (Table 3). However, we observed a trend toward an accuracy-related pattern (i.e., correct rejects > false alarms and hits > misses) in pIPS, resembling the pattern in the beta band. This is consistent with a conjoined increase of persistent beta and gamma band activity in the lateral intraparietal area of the macaque before delayed saccades (Pesaran et al. 2002). Surprisingly, we also found a trend toward an accuracy-related pattern of opposite sign (i.e., false alarms > correct rejects and misses > hits) in dlPFC. Average CPs were 0.49 (target absent) and 0.54 (target present) in pIPS, 0.52 (absent) and 0.46 (present) in dlPFC. In sum, the present data provide no evidence for the idea that gamma band activity in the human dorsal visual pathway reflects the perception of coherent visual motion near detection threshold. Rather, they show that endogenous fluctuations of beta band activity in this pathway during motion viewing predict the *accuracy* of subsequent detection reports.

DISCUSSION

We have studied the relationship between parietal and prefrontal population activity and behavioral performance in a visual motion detection task in humans. MEG activity in the 12- to 24-Hz (beta) frequency range was consistently larger before correct than before incorrect behavioral choices. This performance-predictive activity was not evident in the prestimulus baseline and built up slowly during motion viewing. It was most strongly expressed in prefrontal and posterior parietal cortex, but to a lesser degree also in area MT+. The performance-related and stimulus-induced modulations of MEG activity had different spectral and spatial distributions, and their amplitudes were uncorrelated within each area. Importantly, 12- to 24-Hz activity in MT+, posterior intraparietal sulcus, and dorsolateral prefrontal cortex predicted the *accuracy*, but not the *content*, of subjects' perceptual reports on single trials.

The lack of predictive prestimulus activity in the present study seems to be at odds with previously reported effects of such predictive fMRI activity in visual cortex (Ress et al. 2000; Sapir et al. 2005) and parietal MEG power in the low-frequency (alpha and beta) range (Linkenkaer-Hansen et al. 2004) preceding stimulus onset in detection and discrimination tasks. Several features of our experimental protocol aimed at controlling subjects' attentional baseline state and minimizing the contribution of occasional attention lapses on the subsequent perceptual judgment. First, trials were presented in rapid succession within each block, forcing subjects to maintain a steady level of alertness. Second, the random dot patterns had maximal contrast, eliminating uncertainty about the target position and capturing subjects' attention immediately after stimulus onset. Third, stimuli were presented for a long duration, which reduced the impact of occasional attention lapses before stimulus onset on the perceptual judgments. In addition, we did not explicitly cue subjects to attend to a particular location or visual feature before the onset of the random-dot patterns inducing preparatory activity in the dorsal pathway (Corbetta and Shulman 2002; Sapir et al. 2005). All of these factors might account for the lack of predictive prestimulus activity in the present study. This lack suggests that the process underlying the performance-related activity during motion viewing does not reflect slow baseline fluctuations of arousal and/or selective attention on a timescale longer than the duration of a trial. Rather, this activity reflects a process that is specifically linked to stimulus processing and accurate decision making, such as attention, short-term memory, and/or confidence.

It is well established that the cortex engages in rhythmic population activity in different frequency ranges, depending on the gross brain state (Steriade 2000; Wang 2003); however, the specific functional role of such band-limited activity in sensory processing is less clear. Stimulus-dependent and attentional modulation of local field activity in visual cortex have predominantly been observed in the gamma band (Brosch et al. 1997; Fries et al. 2001; Gray and Singer 1989; Gruber et al. 1999; Henrie and Shapley 2005; Liu and Newsome 2006; Siegel and König 2003; Siegel et al. 2007). The attentional modulation of gamma band responses predicts behavioral performance in visual tasks above detection threshold (Taylor et al. 2005; Womelsdorf et al. 2006). Persistent gamma band activity in parietal cortex predicts the direction of upcoming saccades (Pesaran et al. 2002). By contrast, changes of alpha and beta band activity in cortex have been commonly interpreted as a signature of "cortical deactivation" (e.g., Pfurtscheller and Lopes da Silva 1999). This concept is consistent with the commonly observed strong stimulus-induced suppression of MEG power in the range from about 4 to about 50 Hz in visual and parietal cortex (see also Hoogenboom et al. 2005; Siegel et al. 2007), but inconsistent with the robust performance-related *increase* of 12- to 24-Hz (beta band) activity throughout the dorsal pathway observed in the present study. This apparent discrepancy can be explained by two separate components of the stimulus-induced beta band activity: a strong and unspecific global component and a subtle performance-related component. Visual stimulation presumably decreases low-frequency activity across a large group of task-unrelated neurons, producing large extracranial signals. By contrast, a comparably small pool of neurons in each processing stage of the dorsal

Downloaded from jn.physiology.org on July 27, 2007

pathway, which contributes to the perceptual decision process, might engage in coherent beta band oscillations (Kopell et al. 2000). This, in turn, might lead to small increases of population activity in this frequency range within each processing stage. The different spatial and spectral signatures and the lack of correlation between the two components of the beta band response demonstrated here strongly suggest that they indeed have different neuronal generators.

The behavioral significance of increases in beta band activity for attentive visual processing is consistent with previous studies in macaques and humans. In macaque V1 such increases correlate with perceptual reports during bistable stimulus viewing (Gail et al. 2004; Wilke et al. 2006). Beta band activity in macaque extrastriate visual cortex and lateral intraparietal area correlates with visual working memory (Pesaran et al. 2002; Tallon-Baudry et al. 2004). Synchronization of MEG activity over human frontal and parietal cortex in the beta band is larger before hits than before misses in the "attentional blink" protocol (Gross et al. 2004). By contrast, the lack of percept-related gamma band activity in the present data is inconsistent with percept-related modulations of local field activity in the gamma band observed in macaque MT during fine speed discrimination (Liu and Newsome 2006) and in macaque V4 during the suppression of salient target patterns (Wilke et al. 2006). In both studies, target stimuli were at or close to maximal strength (motion coherence or contrast). There are at least two explanations for this discrepancy. First, percept-related modulations of gamma band field activity in near-threshold tasks might be too small, or confined to too small neuronal groups, to be detectable at the scalp level. Second, gamma band activity might not be related to perception of visual stimuli near detection threshold: Response synchronization in the gamma band might contribute to the representation of stimulus strength only at high levels, at which firing rates tend to saturate (Henrie and Shapley 2005). In line with this idea, gamma band MEG activity in human motion-sensitive cortical visual areas is tightly correlated with visual motion coherence only above detection threshold (Siegel et al. 2007). Furthermore, in the present data, we observed a trend toward an accuracy-related modulation (correct rejects $>$ false alarms) in the gamma band in parietal cortex, arguing against a link to the perceptual representation of near-threshold stimuli. However, there may have occurred a percept-related modulation in MT+ below the sensitivity of our measurements.

The firing rates of single units in macaque MT (Britten et al. 1996; Uka and DeAngelis 2004; Williams et al. 2003), lateral intraparietal area (Cook and Maunsell 2002; Shadlen and Newsome 2001; Williams et al. 2003), and dorsolateral prefrontal cortex (Kim and Shadlen 1999) predict monkeys' behavioral reports about noisy and ambiguous visual motion signals. Importantly, these spike-rate fluctuations predict the content of perceptual choices. Thus large-scale field activity in the beta band seems to provide qualitatively different information about perceptual decision processes than average firing rates: It does not predict the content of the upcoming choice and thus is not involved in the *representation* of the sensory stimulus (or a derived decision variable). Rather it indexes the *computations* transforming such representations into actions (deCharms and Zador 2000; Salinas and Sejnowski 2001). Specifically, coherent beta band activity might regulate the flow of motion representations through the dorsal visual pathway (Salinas and Sejnowski 2001). Fluctuations of the strength of this activity then cause fluctuations of the efficiency of signal flow and thus of decision accuracy. Alternatively, beta band activity in the dorsal pathway may reflect synaptic reverberation: Such reverberation may underlie the temporal integration of motion signals in cortical decision circuits (Wang et al. 2001, 2003) and may produce periodic temporal structure in neural population activity (Pesaran et al. 2002; Tallon-Baudry et al. 2004). In this context, it is noteworthy that the cortical distribution of performance-predictive MEG activity in the present study corresponds closely with the distribution of performance fMRI activity during the delay of a visual short-term memory task (Pessoa et al. 2002).

To conclude, we demonstrated that the trial-to-trial fluctuations of band-limited cortical population activity in several key stages of the human dorsal visual pathway predict the trial-to-trial fluctuations of behavioral motion detection. Specifically, we established that beta band activity in this pathway predicts the accuracy, and not the content, of simple perceptual decisions.

ACKNOWLEDGMENTS

We thank three anonymous reviewers for constructive comments on this manuscript.

Present addresses: T. H. Donner, Department of Psychology and Center for Neural Science, New York University, New York, NY; M. Siegel, The Picower Institute for Learning and Memory, Department of Brain and Cognitive Sciences, Massachusetts Institute of Technology, Cambridge, MA; M. Bauer, Max Planck Institute for Human Development, Berlin, Germany.

GRANTS

This study was supported by grants from the Deutsche Forschungsgemeinschaft to A. K. Engel; the Danish Research Council to R. Oostenveld; Netherlands Organization for Scientific Research to P. Fries; Human Frontier Science Program to P. Fries; European Commission to A. K. Engel; Volkswagen Foundation to A. K. Engel and P. Fries; and the Lungwitz Foundation to A. K. Engel, M. Siegel, and T. H. Donner.

REFERENCES

Arieli A, Sterkin A, Grinvald A, Aertsen A. Dynamics of ongoing activity: explanation of the large variability in evoked cortical responses. *Science* 273: 1868–1871, 1996.

Beck DM, Rees G, Frith CD, Lavie N. Neural correlates of change detection and change blindness. *Nat Neurosci* 4: 645–650, 2001.

Braddick OJ, O'Brien JM, Wattam-Bell J, Atkinson J, Turner R. Form and motion coherence activate independent, but not dorsal/ventral segregated, networks in the human brain. *Curr Biol* 10: 731–734, 2000.

Britten KH, Newsome WT, Shadlen MN, Celebrini S, Movshon JA. A relationship between behavioral choice and the visual responses of neurons in macaque MT. *Vis Neurosci* 13: 87–100, 1996.

Brosch M, Bauer R, Eckhorn R. Stimulus-dependent modulations of correlated high-frequency oscillations in cat visual cortex. *Cereb Cortex* 7: 70–76, 1997.

Buracas GT, Zador AM, DeWeese MR, Albright TD. Efficient discrimination of temporal patterns by motion-sensitive neurons in primate visual cortex. *Neuron* 20: 959–969, 1998.

Carandini M. Amplification of trial-to-trial response variability by neurons in visual cortex. *PLoS Biol* 2: E264, 2004.

Cook EP, Maunsell JH. Dynamics of neuronal responses in macaque MT and VIP during motion detection. *Nat Neurosci* 5: 985–994, 2002.

Corbetta M, Shulman GL. Control of goal-directed and stimulus-driven attention in the brain. *Nat Rev Neurosci* 3: 201–215, 2002.

deCharms RC, Zador A. Neural representation and the cortical code. *Annu Rev Neurosci* 23: 613–647, 2000.

Donner T, Ketterman A, Diesch E, Ostendorf F, Villringer A, Brandt SA. Involvement of the human frontal eye field and multiple parietal areas in covert visual selection during conjunction search. *Eur J Neurosci* 12: 3407–3414, 2000.

Dumoulin SO, Bittar RG, Kabani NJ, Baker CL, Jr, Le Goualher G, Bruce Pike G, Evans AC. A new anatomical landmark for reliable identi-

Downloaded from jn.physiology.org on July 27, 2007

fication of human area V5/MT: a quantitative analysis of sulcal patterning. *Cereb Cortex* 10: 454–463, 2000.
Efron B, Tibshirani R. *An Introduction to the Bootstrap*. Boca Raton, FL: Chapman & Hall/CRC, 1998.
Felleman DJ, Van Essen DC. Distributed hierarchical processing in the primate cerebral cortex. *Cereb Cortex* 1: 1–47, 1991.
Fries P, Reynolds JH, Rorie AE, Desimone R. Modulation of oscillatory neuronal synchronization by selective visual attention. *Science* 291: 1560–1563, 2001.
Gail A, Brinksmeyer HJ, Eckhorn R. Perception-related modulations of local field potential power and coherence in primary visual cortex of awake monkey during binocular rivalry. *Cereb Cortex* 14: 300–313, 2004.
Gold JI, Shadlen MN. Neural computations that underlie decisions about sensory stimuli. *Trends Cogn Sci* 5: 10–16, 2001.
Graham NVS. *Visual Pattern Analyzers*. New York: Oxford Univ. Press, 1989.
Gray CM, Singer W. Stimulus-specific neuronal oscillations in orientation columns of cat visual cortex. *Proc Natl Acad Sci USA* 86: 1698–1702, 1989.
Green DM, Swets JA. *Signal Detection Theory and Psychophysics*. New York: Wiley, 1966.
Gross J, Kujala J, Hamalainen M, Timmermann L, Schnitzler A, Salmelin R. Dynamic imaging of coherent sources: studying neural interactions in the human brain. *Proc Natl Acad Sci USA* 98: 694–699, 2001.
Gross J, Schmitz F, Schnitzler I, Kessler K, Shapiro K, Hommel B, Schnitzler A. Modulation of long-range neural synchrony reflects temporal limitations of visual attention in humans. *Proc Natl Acad Sci USA* 101: 13050–13055, 2004.
Gruber T, Muller MM, Keil A, Elbert T. Selective visual-spatial attention alters induced gamma band responses in the human EEG. *Clin Neurophysiol* 110: 2074–2085, 1999.
Hamalainen M, Hari R, Ilmoniemi RJ, Knuutila J, Lounasmaa OV. Magnetoencephalography—theory, instrumentation, and applications to noninvasive studies of the working human brain. *Rev Modern Phys* 65: 413–497, 1993.
Heggelund P, Albus K. Response variability and orientation discrimination of single cells in striate cortex of cat. *Exp Brain Res* 32: 197–211, 1978.
Henrie JA, Shapley R. LFP power spectra in V1 cortex: the graded effect of stimulus contrast. *J Neurophysiol* 94: 479–490, 2005.
Huang MX, Mosher JC, Leahy RM. A sensor-weighted overlapping-sphere head model and exhaustive head model comparison for MEG. *Phys Med Biol* 44: 423–440, 1999.
Huk AC, Dougherty RF, Heeger DJ. Retinotopy and functional subdivision of human areas MT and MST. *J Neurosci* 22: 7195–7205, 2002.
Kim JN, Shadlen MN. Neural correlates of a decision in the dorsolateral prefrontal cortex of the macaque. *Nat Neurosci* 2: 176–185, 1999.
Kopell N, Ermentrout GB, Whittington MA, Traub RD. Gamma rhythms and beta rhythms have different synchronization properties. *Proc Natl Acad Sci USA* 97: 1867–1872, 2000.
Kranczioch C, Debener S, Schwarzbach J, Goebel R, Engel AK. Neural correlates of conscious perception in the attentional blink. *Neuroimage* 24: 704–714, 2005.
Leopold DA, Murayama Y, Logothetis NK. Very slow activity fluctuations in monkey visual cortex: implications for functional brain imaging. *Cereb Cortex* 13: 422–433, 2003.
Linkenkaer-Hansen K, Nikulin VV, Palva S, Ilmoniemi RJ, Palva J. Pre-stimulus oscillations enhance psychophysical performance in humans. *J Neurosci* 24: 10186–10190, 2004.
Liu J, Newsome WT. Local field potential in cortical area MT: stimulus tuning and behavioral correlations. *J Neurosci* 26: 7779–7790, 2006.
Makeig S, Inlow M. Lapses in alertness: coherence of fluctuations in performance and EEG spectrum. *Electroencephalogr Clin Neurophysiol* 86: 23–35, 1993.
Marois R, Yi DJ, Chun MM. The neural fate of consciously perceived and missed events in the attentional blink. *Neuron* 41: 465–472, 2004.
McKeeff TJ, Tong F. The timing of perceptual decisions for ambiguous face stimuli in the human ventral visual cortex. *Cereb Cortex* 17: 669–678, 2007.
Mitra PP, Pesaran B. Analysis of dynamic brain imaging data. *Biophys J* 76: 691–708, 1999.
Parker AJ, Newsome WT. Sense and the single neuron: probing the physiology of perception. *Annu Rev Neurosci* 21: 227–277, 1998.
Pesaran B, Pezaris JS, Sahani M, Mitra PP, Andersen RA. Temporal structure in neuronal activity during working memory in macaque parietal cortex. *Nat Neurosci* 5: 805–811, 2002.
Pessoa L, Gutierrez E, Bandettini P, Ungerleider L. Neural correlates of visual working memory: fMRI amplitude predicts task performance. *Neuron* 35: 975–987, 2002.
Pfurtscheller G, Lopes da Silva FH. Event-related EEG/MEG synchronization and desynchronization: basic principles. *Clin Neurophysiol* 110: 1842–1857, 1999.
Rees G, Friston K, Koch C. A direct quantitative relationship between the functional properties of human and macaque V5. *Nat Neurosci* 3: 716–723, 2000.
Ress D, Backus BT, Heeger DJ. Activity in primary visual cortex predicts performance in a visual detection task. *Nat Neurosci* 3: 940–945, 1999.
Ress D, Heeger DJ. Neuronal correlates of perception in early visual cortex. *Nat Neurosci* 6: 414–420, 2003.
Salinas E, Sejnowski TJ. Correlated neuronal activity and the flow of neural information. *Nat Rev Neurosci* 2: 539–550, 2001.
Sapir A, d'Avossa G, McAvoy M, Shulman GL, Corbetta M. Brain signals for spatial attention predict performance in a motion discrimination task. *Proc Natl Acad Sci USA* 102: 17810–17815, 2005.
Shadlen MN, Britten KH, Newsome WT, Movshon JA. A computational analysis of the relationship between neuronal and behavioral responses to visual motion. *J Neurosci* 16: 1486–1510, 1996.
Shadlen MN, Newsome WT. Neural basis of a perceptual decision in the parietal cortex (area LIP) of the rhesus monkey. *J Neurophysiol* 86: 1916–1936, 2001.
Shulman GL, Ollinger JM, Linenweber M, Petersen SE, Corbetta M. Multiple neural correlates of detection in the human brain. *Proc Natl Acad Sci USA* 98: 313–318, 2001.
Siegel M, Donner TH, Oostenveld R, Fries P, Engel AK. High-frequency activity in human visual cortex is modulated by visual motion strength. *Cereb Cortex* 17: 732–741, 2007.
Siegel M, König P. A functional gamma-band defined by stimulus-dependent synchronization in area 18 of awake behaving cats. *J Neurosci* 23: 4251–4260, 2003.
Steriade M. Corticothalamic resonance, states of vigilance and mentation. *Neuroscience* 101: 243–276, 2000.
Summerfield C, Egner T, Mangels J, Hirsch J. Mistaking a house for a face: neural correlates of misperception in healthy humans. *Cereb Cortex* 16: 500–508, 2006.
Talairach J, Tournoux P. *Co-planar Stereotaxic Atlas of the Human Brain: Three-Dimensional Proportional System: An Approach to Cerebral Imaging*. New York: Thieme Medical Publishers, 1988.
Tallon-Baudry C, Bertrand O. Oscillatory gamma activity in humans and its role in object representation. *Trends Cogn Sci* 3: 151–162, 1999.
Tallon-Baudry C, Mandon S, Freiwald WA, Kreiter AK. Oscillatory synchrony in the monkey temporal lobe correlates with performance in a visual short-term memory task. *Cereb Cortex* 14: 713–720, 2004.
Taylor K, Mandon S, Freiwald WA, Kreiter AK. Coherent oscillatory activity in monkey area V4 predicts successful allocation of attention. *Cereb Cortex* 15: 1424–1437, 2005.
Thiele A, Distler C, Hoffmann KP. Decision-related activity in the macaque dorsal visual pathway. *Eur J Neurosci* 11: 2044–2058, 1999.
Uka T, DeAngelis GC. Contribution of area MT to stereoscopic depth perception: choice-related response modulations reflect task strategy. *Neuron* 22: 297–310, 2004.
Ungerleider LG, Haxby JV. "What" and "where" in the human brain. *Curr Opin Neurobiol* 4: 157–165, 1994.
Van Veen BD, van Drongelen W, Yuchtman M, Suzuki A. Localization of brain electrical activity via linearly constrained minimum variance spatial filtering. *IEEE Trans Biomed Eng* 44: 867–880, 1997.
Wang XJ. Synaptic reverberation underlying mnemonic persistent activity. *Trends Neurosci* 24: 455–463, 2001.
Wang XJ. Probabilistic decision making by slow reverberation in cortical circuits. *Neuron* 36: 955–968, 2002.
Wang XJ. Neural oscillations. In: *Encyclopedia of Cognitive Science*, edited by Nadel L. London: Macmillan, 2003, p. 272–280.
Wilke M, Logothetis NK, Leopold DA. Local field potential reflects perceptual suppression in monkey visual cortex. *Proc Natl Acad Sci USA* 103: 17507–17512, 2006.
Williams PE, Mechler F, Gordon J, Shapley R, Hawken MJ. Entrainment to video displays in primary visual cortex of macaque and humans. *J Neurosci* 24: 8278–8288, 2004.
Williams ZM, Elfar JC, Eskandar EN, Toth LJ, Assad JA. Parietal activity and the perceived direction of ambiguous apparent motion. *Nat Neurosci* 6: 616–623, 2003.
Womelsdorf T, Fries P, Mitra PP, Desimone R. Gamma-band synchronization in visual cortex predicts speed of change detection. *Nature* 439: 733–736, 2006.

Downloaded from jn.physiology.org on July 27, 2007